Head-to-Head Evaluation of ^{18}F-FES and ^{18}F-FDG PET/CT in Metastatic Invasive Lobular Breast Cancer

Gary A. Ulaner[1,2], Komal Jhaveri[3,4], Sarat Chandarlapaty[3,4], Vaios Hatzoglou[2,5], Christopher C. Riedl[2,5], Jason S. Lewis[2,5], and Audrey Mauguen[6]

[1]Molecular Imaging and Therapy, Hoag Family Cancer Institute, Newport Beach, California; [2]Department of Radiology, Memorial Sloan Kettering Cancer Center, New York, New York; [3]Department of Medicine, Memorial Sloan Kettering Cancer Center, New York, New York; [4]Department of Medicine, Weill Cornell Medical College, New York, New York; [5]Department of Radiology, Weill Cornell Medical College, New York, New York; and [6]Department of Epidemiology and Biostatistics, Memorial Sloan Kettering Cancer Center, New York, New York

Invasive lobular carcinoma (ILC) demonstrates lower conspicuity on ^{18}F-FDG PET than the more common invasive ductal carcinoma. Other molecular imaging methods may be needed for evaluation of this malignancy. As ILC is nearly always (95%) estrogen receptor (ER)–positive, ER-targeting PET tracers such as 16α-^{18}F-fluoroestradiol (^{18}F-FES) may have value. We reviewed prospective trials at Memorial Sloan Kettering Cancer Center using ^{18}F-FES PET/CT to evaluate metastatic ILC patients with synchronous ^{18}F-FDG and ^{18}F-FES PET/CT imaging, which allowed a head-to-head comparison of these 2 PET tracers. **Methods:** Six prospective clinical trials using ^{18}F-FES PET/CT in patients with metastatic breast cancer were performed at Memorial Sloan Kettering Cancer Center from 2008 to 2019. These trials included 92 patients, of whom 14 (15%) were of ILC histology. Seven of 14 patients with ILC had ^{18}F-FDG PET/CT performed within 5 wk of the research ^{18}F-FES PET/CT and no intervening change in management. For these 7 patients, the ^{18}F-FES and ^{18}F-FDG PET/CT studies were analyzed to determine the total number of tracer–avid lesions, organ systems of involvement, and SUV_{max} of each organ system for both tracers. **Results:** In the 7 comparable pairs of scans, there were a total of 254 ^{18}F-FES–avid lesions (SUV_{max}, 2.6–17.9) and 111 ^{18}F-FDG–avid lesions (SUV_{max}, 3.3–9.9) suggestive of malignancy. For 5 of 7 (71%) ILC patients, ^{18}F-FES PET/CT detected more metastatic lesions than ^{18}F-FDG PET/CT. In the same 5 of 7 patients, the SUV_{max} of ^{18}F-FES–avid lesions was greater than the SUV_{max} of ^{18}F-FDG–avid lesions. One patient had ^{18}F-FES–avid metastases with no corresponding ^{18}F-FDG–avid metastases. There were no patients with ^{18}F-FDG–avid distant metastases without ^{18}F-FES–avid distant metastases, although in one patient liver metastases were evident on ^{18}F-FDG but not on ^{18}F-FES PET. **Conclusion:** ^{18}F-FES PET/CT compared favorably with ^{18}F-FDG PET/CT for detection of metastases in patients with metastatic ILC. Larger prospective trials of ^{18}F-FES PET/CT in ILC should be considered to evaluate ER-targeted imaging for clinical value in patients with this histology of breast cancer.

Key Words: lobular; breast cancer; ^{18}F-FES; ^{18}F-FDG, PET/CT

J Nucl Med 2021; 62:326–331
DOI: 10.2967/jnumed.120.247882

PET/CT with ^{18}F-FDG plays an important role in the management of patients with breast cancer (*1,2*). The impact of ^{18}F-FDG PET/CT in patients with breast cancer differs between the most common histology of breast cancer, invasive ductal carcinoma (80% of cases) and the second most common histology, invasive lobular carcinoma (ILC, 10%–15% of cases) (*3,4*). Because of distinct molecular and pathologic features (*5,6*), including lower cellular density per unit volume, ILC is more difficult to detect on imaging, including mammography, ultrasound, MRI, and ^{18}F-FDG PET/CT (*7–16*). Both primary and metastatic ILC demonstrates lower SUVs on ^{18}F-FDG PET than do comparable invasive ductal carcinoma tumors (*11–16*). In addition, ILC differs from invasive ductal carcinoma in patterns of metastatic spread (*17–20*). Given these differences, ^{18}F-FDG PET/CT may be less suited for evaluation of ILC than for evaluation of invasive ductal carcinoma (*16*).

ILC also differs from invasive ductal carcinoma in receptor expression. In particular, ILC is nearly always (95%) estrogen receptor (ER)–positive (*5,21,22*), raising the possibility of increased utility of ER-targeting PET tracers for patients with ILC. 16α-^{18}F-fluoroestradiol (^{18}F-FES) is an ER-targeting PET tracer with high sensitivity and specificity for detection of ER-positive tumors (*23–27*). ^{18}F-FES has been used as a predictive biomarker (*28–31*) to demonstrate ER heterogeneity (*32,33*), assess the pharmacokinetics of ER-targeted agents (*34*), measure residual ER during endocrine therapy (*35*), and determine the biologic optimal dose of novel ER-targeted drugs (*36*).

We hypothesized that because of high ER positivity, ^{18}F-FES PET/CT may compare favorably with ^{18}F-FDG PET/CT in patients with ILC. Prospective trials have been conducted at Memorial Sloan Kettering using ^{18}F-FES PET/CT to assist in determining the dose of novel ER-targeted drugs. We reviewed these trials for patients with ILC who underwent ^{18}F-FDG PET/CT within 5 wk of the research ^{18}F-FES PET/CT and had no intervening change in management. Here, we report this head-to-head comparison of ^{18}F-FES and ^{18}F-FDG PET/CT in patients with metastatic ILC.

MATERIALS AND METHODS

Patients

This retrospective evaluation of prospective clinical trials was performed in compliance with the Health Insurance Portability and Accountability Act and with Institutional Review Board approval. All patients provided written informed consent. Six prospective clinical trials using ^{18}F-FES PET/CT in patients with breast cancer (NCT01823835,

Received Apr. 21, 2021; revision accepted Jun. 15, 2020.
For correspondence or reprints contact: Gary A. Ulaner, Molecular Imaging and Therapy, Hoag Family Cancer Institute, Newport Beach, CA 92663.
E-mail: gary.ulaner@hoag.org
Published online Jul. 17, 2020.

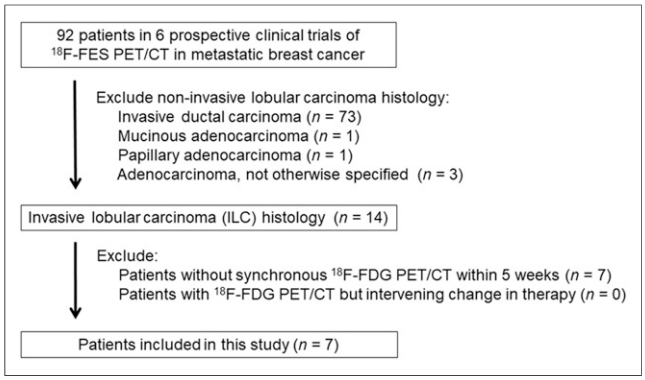

FIGURE 1. STARD diagram for patients screened in this study.

NCT01916122, NCT02316509, NCT02734615, NCT03284957, and NCT03332797) were reviewed for patients with metastatic invasive lobular breast cancer and standard-of-care ^{18}F-FDG PET/CT performed within 5 wk of research ^{18}F-FES PET/CT and who had no change in therapeutic management between scans. Both the research ^{18}F-FES PET/CT and the standard-of-care ^{18}F-FDG PET/CT studies were performed before therapy, without intervening change in patient management.

Electronic medical records were reviewed for age at ^{18}F-FES PET/CT, sex, and receptor status (ER, progesterone receptor, and human growth factor receptor 2), as well as number of days between the ^{18}F-FES and ^{18}F-FDG PET/CT scans.

PET/CT Imaging and Interpretation

The ^{18}F-FDG PET/CT and ^{18}F-FES PET/CT studies were reinterpreted by a radiologist dually boarded in diagnostic radiology and nuclear medicine with 15 y of PET/CT experience, including experience with both agents.

The ^{18}F-FES PET/CT acquisition was standardized in all studies according to a registered clinical trial (NCT01916122). ^{18}F-FES was manufactured by the Radiochemistry and Imaging Probe Core at Memorial Sloan Kettering Cancer Center using a modified version of a published work by Knott et al. (*37*). Each patient was administered approximately 185 MBq (5 mCi) of ^{18}F-FES intravenously, followed by a 60-min uptake period. PET/CT scans were acquired supine from the base of the skull to the mid thigh along with low-dose CT scans. Attenuation-corrected images were reviewed on a PACS workstation (GE Healthcare). Physiologic ^{18}F-FES avidity was expected in the liver, bowel, kidney, and bladder. ^{18}F-FES avidity was considered abnormal when it was focal and not considered physiologic.

For ^{18}F-FDG PET/CT examinations, ^{18}F-FDG was obtained from a commercial source. Patients fasted for at least 6 h before ^{18}F-FDG administration. Each patient was injected intravenously with 444–555 MBq (12–15 mCi) of ^{18}F-FDG when plasma glucose was less than 200 mg/dL, followed by a 60-min uptake period. PET/CT scans were acquired supine from the base of the skull to the mid thigh along with low-dose CT scans. Attenuation-corrected images were reviewed on a PACS workstation. ^{18}F-FDG avidity was considered abnormal when it was focal and not considered physiologic or inflammatory.

For both examinations, the organ systems with disease involvement, the number of disease foci in each organ system, and the SUV_{max} for lesions were recorded. SUV_{max} was determined by placement of regions of interest around the lesions with the greatest avidity. As lesions had different ^{18}F-FES and ^{18}F-FDG avidity, different lesions were sometimes selected as the most avid for each study. Liver background SUV_{max} and SUV_{mean} were determined by placement of regions of interest over a 1-cm^3 volume of the right lobe of the liver.

Statistics

Results were described using median and range. To assess whether the distribution of the number of lesions or the SUV_{max} was higher with ^{18}F-FES PET than with ^{18}F-FDG PET, 1-sided Wilcoxon signed-rank

TABLE 1
Malignancy Seen on ^{18}F-FES and ^{18}F-FDG PET/CT in the 7 Patients

	Patient 1, 67 y old, 30 d between scans		Patient 2, 64 y old, 11 d between scans		Patient 3, 67 y old, 13 d between scans		Patient 4, 66 y old, 16 d between scans		Patient 5, 48, y old, 30 d between scans		Patient 6, 54 y old, 35 d between scans		Patient 7, 69 y old, 19 d between scans	
Parameter	^{18}F-FES	^{18}F-FDG	^{18}F-FES	^{18}F-FDG	^{18}F-FES	^{18}F-FDG	^{18}F-FES	^{18}F-FDG	^{18}F-FES	^{18}F-FDG	^{18}F-FES	^{18}F-FDG	^{18}F-FES	^{18}F-FDG
Bone														
Foci (*n*)	68	2	146	56	3	2	14	8	2	0	4	16	16	6
SUV_{max}	11.4	3.5	17.9	5.7	14.8	3.6	10.2	5.8	3.7	NA	2.6	5.0	7.9	9.9
Location*	L4 VB	L ilium	R femur	R femur	L3 VB	L3 VB	Sac	Sac	R ilium	NA	R acet	Sac	L acet	L1 VB
Breast														
Foci (*n*)					1	1								
SUV_{max}					6.5	3.3								
Liver														
Foci (*n*)													0	20
SUV_{max}													NA	5.9
bg SUV_{max}	13.8	2.5	15.4	3.1	15.4	2.2	22.9	2.8	12.5	2.2	14.3	3.8	17.0	3.5
bg SUV_{mean}	10.6	2.2	13.8	2.8	13.9	1.9	20.3	2.6	11.7	2.0	12.4	3.5	15.0	3.1

*Location of osseous lesions (noted by red arrows in Fig. 1) demonstrating SUV_{max}.
VB = vertebral body; sac = sacrum; NA = not applicable; acet = acetabulum; bg = liver background.

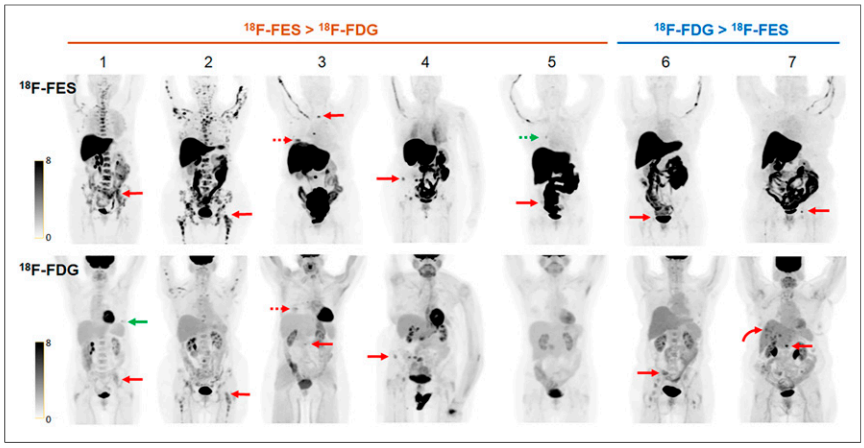

FIGURE 2. Comparison of ^{18}F-FES PET and ^{18}F-FDG PET in 7 patients with metastatic ILC. Images are maximum-intensity projections from ^{18}F-FES PET scans and ^{18}F-FDG PET scans within 5 wk. In first 5 patients, ^{18}F-FES PET detected more metastatic lesions and demonstrated higher SUVs for metastatic lesions than did ^{18}F-FDG. In patients 1–5, more osseous metastases (solid red arrows) were seen on ^{18}F-FES PET than on ^{18}F-FDG PET. In particular, for patient 5, osseous disease was detected on ^{18}F-FES PET but was not apparent on ^{18}F-FDG. In patient 3, known recurrence in breast (dashed red arrows) demonstrated greater SUV_{max} on ^{18}F-FES than on ^{18}F-FDG. In patient 1, ^{18}F-FDG avidity around breast implant (green arrow) was probably benign. In patient 5, right hilar focus was of unclear etiology (green arrow). In last 2 patients, ^{18}F-FDG PET detected more metastatic lesions than did ^{18}F-FES PET. In patient 6, more osseous metastases (arrows) were seen on ^{18}F-FDG PET than on ^{18}F-FES PET. In patient 7, more osseous metastases (straight red arrows) were seen on ^{18}F-FES PET, but multiple liver metastases (curved red arrow) were seen only on ^{18}F-FDG PET.

tests for paired data were used. To account for the small sample size, results with a P value of less than 0.10 were considered statistically significant.

RESULTS

Patients

Ninety-two patients with breast cancer underwent ^{18}F-FES PET/CT as part of 6 prospective clinical trials. Seventy-eight (85%) were excluded for non-ILC histology. Seven (8%) were excluded for no comparison ^{18}F-FDG PET/CT. The result was 7 evaluable patients. A STARD (Standards for Reporting of Diagnostic Accuracy Studies) diagram for patient selection is presented in Figure 1. The 7 patients were all women with ER-positive, progesterone receptor–positive, and human growth factor receptor 2–negative ILC. The median age was 66 y (range, 48–69 y). For all patients, the ^{18}F-FDG PET/CT was performed before the ^{18}F-FES PET/CT. The median time between scans was 19 d (range, 11–35 d).

^{18}F-FES PET/CT

All 7 patients demonstrated ^{18}F-FES–avid lesions consistent with metastases (Table 1). All demonstrated osseous metastases, and one demonstrated a biopsy-proven breast recurrence. In total, 253 ^{18}F-FES–avid osseous lesions were seen. The ^{18}F-FES SUV_{max} range for osseous lesions among the 7 patients was 2.6–17.9 (median, 10.2). There was a focus representing breast recurrence in patient 3, with an ^{18}F-FES SUV_{max} of 6.5. Patient 5 demonstrated a focus in the right lung hilum (SUV_{max}, 3.6), without a correlate on CT, of unclear etiology. This focus was not included in the lesions suggestive of malignancy, as the right hilum is unlikely to be a site of nodal metastases in a breast cancer patient without axillary or internal mammary nodal metastases. No other organ systems were found to have suggestive ^{18}F-FES–avid foci.

^{18}F-FDG PET/CT

Six of 7 patients demonstrated ^{18}F-FDG–avid lesions consistent with metastases (Table 1). Six demonstrated ^{18}F-FDG–avid osseous metastases, 1 demonstrated an ^{18}F-FDG–avid, biopsy-proven breast recurrence, and 1 demonstrated ^{18}F-FDG–avid hepatic metastases. In total, 90 ^{18}F-FDG–avid osseous lesions were seen. The ^{18}F-FDG SUV_{max} range for osseous lesions was 3.5–9.9 (median, 5.3). There was 1 focus representing breast recurrence in patient 3 (the same lesion as detected on ^{18}F-FES PET/CT), with an SUV_{max} of 3.3. Patient 7 demonstrated 20 ^{18}F-FDG–avid hepatic metastases with an SUV_{max} of 5.9. Patient 1 demonstrated ^{18}F-FDG avidity that was probably benign, adjacent to a breast implant. No other organ systems were found to have suggestive ^{18}F-FDG–avid foci.

Comparison of ^{18}F-FES and ^{18}F-FDG PET/CT

In 5 of 7 patients (71%), ^{18}F-FES PET/CT detected more metastatic lesions than ^{18}F-FDG PET/CT (Table 1; Fig. 2). In these 5 patients, the SUV_{max} of ^{18}F-FES–avid lesions was greater than the SUV_{max} of ^{18}F-FDG–avid lesions.

In total, 268 osseous lesions were detected by either ^{18}F-FES or ^{18}F-FDG PET. Of 268 lesions, 253 (94%) were ^{18}F-FES–avid, whereas 90 of 268 (34%) were ^{18}F-FDG–avid. ^{18}F-FES PET detected more osseous lesions (median, 14; range, 2–146 lesions) than ^{18}F-FDG (median, 6; range, 0–56, $P = 0.08$). In 6 of 7 patients, more osseous foci were detected on ^{18}F-FES PET than on ^{18}F-FDG PET. In 1 patient, 2 avid osseous metastases were seen on ^{18}F-FES PET, but no avid osseous metastases were detected on ^{18}F-FDG PET (patient 5; Table 1, Fig. 2). This patient had extensive sclerotic osseous lesions on CT (Fig. 3) and known active osseous metastases from a biopsy used to enroll the patient in the prospective clinical trial. Patients could demonstrate heterogeneity of tracer avidity, with

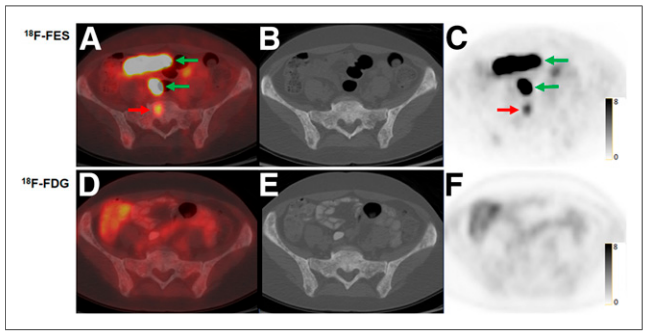

FIGURE 3. Metastatic disease apparent on ^{18}F-FES PET but not on ^{18}F-FDG PET in 48-y-old woman with biopsy-proven metastatic ILC (patient 5). Axial ^{18}F-FES PET/CT (A), CT (B), and ^{18}F-FES PET (C) demonstrate ^{18}F-FES–avid osseous foci (red arrows), consistent with avid malignancy. Physiologic activity was also seen in bowel (green arrows). Axial ^{18}F-FDG PET/CT (D), CT (E), and ^{18}F-FDG PET (F) did not demonstrate any ^{18}F-FDG–avid foci suspected of being malignancy.

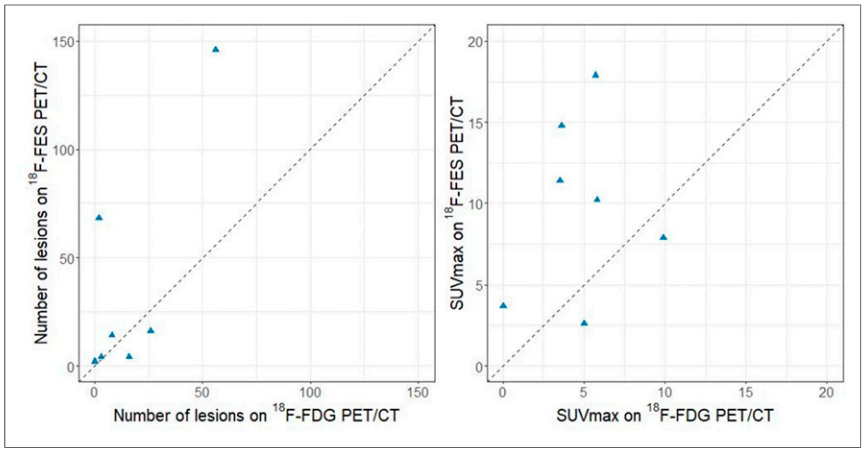

FIGURE 4. Comparison of lesions on ^{18}F-FES PET/CT and ^{18}F-FDG PET/CT in 7 patients with metastatic lobular breast cancer. (Left) Comparison of number of avid lesions suggestive of malignancy. (Right) Comparison of SUV_{max} of suspected lesions. In 5 of 7 patients, more lesions were detected and SUV_{max} was higher on ^{18}F-FES PET/CT than on ^{18}F-FDG PET/CT.

some osseous metastases being avid for both tracers and others being ^{18}F-FES–avid but not ^{18}F-FDG–avid, or vice versa (patient 7; Fig. 2). Therefore, the total number of osseous metastases detected in the study was higher than the total with either tracer alone.

Additionally, 1 patient (patient 7) demonstrated 20 ^{18}F-FDG–avid hepatic metastases that were not apparent on ^{18}F-FES PET (Table 1; Fig. 2). Detection of hepatic metastases is known to be more difficult on ^{18}F-FES PET because of physiologic excretion of ^{18}F-FES by the liver. As expected, in the patients in our study, physiologic liver background was higher on ^{18}F-FES PET than on ^{18}F-FDG PET. The median physiologic liver background ^{18}F-FES SUV_{max} and SUV_{mean} were 15.4 (range, 12.5–22.9) and 13.8 (range, 10.6–20.3), respectively, whereas the median physiologic liver background ^{18}F-FDG SUV_{max} and SUV_{mean} were 2.8 (range, 2.2–3.8) and 2.6 (range, 1.9–3.5), respectively.

Figure 4 depicts the number of lesions detected on ^{18}F-FES PET/CT and ^{18}F-FDG PET/CT in each patient and compares the lesional SUV_{max} for both radiotracers in each patient. Figure 5 graphs SUV_{max} for all lesions in all patients.

DISCUSSION

ILC is a histologic subtype of breast cancer with distinct molecular and imaging characteristics. Novel methods may be needed for optimal visualization of ILC. This study took advantage of prospective trials using ^{18}F-FES to perform a head-to-head comparison between ^{18}F-FES and ^{18}F-FDG PET/CT in patients with metastatic ILC and demonstrated that ^{18}F-FES may compare favorably with ^{18}F-FDG in these patients.

ILC is sometimes thought of as a rare tumor type, but this is a misconception. Although only 15% of all breast malignancies are ILC (*3,38*), 15% of 279,000 breast malignancies a year (*39*) represents 42,000 malignancies. If ILC was its own category of malignancy, it would be the fifth most common malignancy in women, behind only ductal breast cancer, lung, colon/rectum, and uterine cancer (*39*). Thus, ILC is common, and improved imaging of this malignancy could have a major impact on health care.

^{18}F-FES PET is gaining increased recognition as a PET tracer with clinical applicability and has recently been approved by the U.S. Food and Drug Administration for evaluation of ER heterogeneity as EstroTep (Zionexae). This early study suggests that evaluation of metastatic ILC may be a clinical scenario in which ^{18}F-FES PET/CT has clinical utility.

Molecular imaging has demonstrated advantages over anatomic imaging for osseous malignancies. Because the attenuation and density of an osseous lesion must change 30%–50% before being detected on CT (*40*), molecular techniques such as bone scanning and ^{18}F-FDG PET are often more sensitive for detection of osseous malignancy (*41,42*). Because of the limitations of anatomic imaging in osseous lesions, RECIST does not consider osseous lesions without soft-tissue components to be eligible as target lesions (*43*). As the most common site of distant metastasis in ILC is bone (*44*), it is important to have an imaging method that is sensitive for the detection of osseous disease. In this study, ^{18}F-FES PET was more sensitive than ^{18}F-FDG PET for osseous lesions on both a per-lesion and per-patient basis (Table 1). The detection of ^{18}F-FES–avid osseous lesions in ILC can assist with evaluation of the extent of disease and could be considered a method to identify measurable lesions for clinical trials, similar to the recent use of ^{18}F-FDG PET to expand trial eligibility in solid tumors with a predominance of osseous disease (*45*).

The liver is a recognized site of weakness for ^{18}F-FES PET imaging because of physiologic excretion of ^{18}F-FES through the hepatobiliary system. Thus, if ^{18}F-FES PET is used for patient care, the liver will need to be evaluated by an additional method, such as contrast-enhanced CT or MRI.

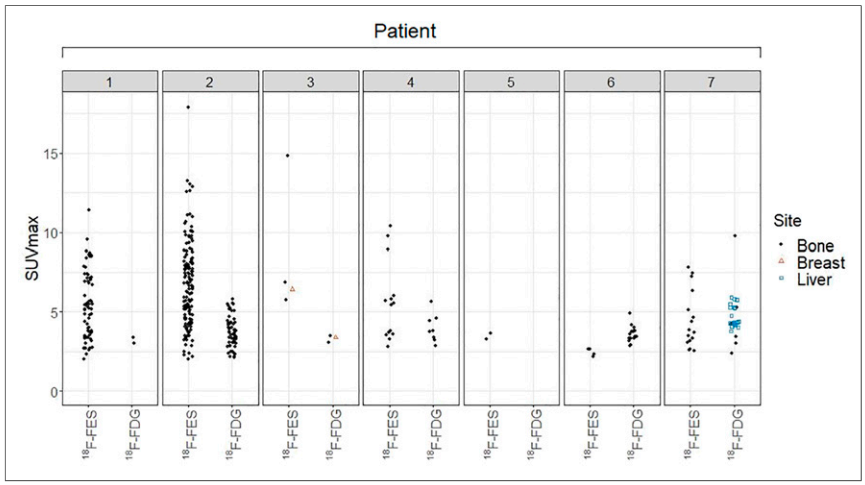

FIGURE 5. Graphical depiction of SUV_{max} for all avid malignancy in all PET/CT scans. There was no ^{18}F-FDG–avid malignancy in patient 5. Most metastases were osseous. Patient 3 had breast lesion. Patient 7 had hepatic metastases seen on ^{18}F-FDG.

Our study had several limitations. The first was the limited number of patients. This study was only an initial comparison of ^{18}F-FES and ^{18}F-FDG PET/CT in patients with metastatic ILC. Because ^{18}F-FES PET/CT is not yet widespread, and because ILC was only recently recognized as a distinct breast cancer subtype requiring alternate methods of molecular imaging (*46–48*), limited numbers of patients are available for analysis. Second, in the patients in this article, ^{18}F-FDG PET was always performed before ^{18}F-FES PET. Thus, there could have been some progression of disease in the 11–35 d between scans. Third, ^{18}F-FDG PET and ^{18}F-FES scans might not have been performed on the same PET/CT scanner. Fourth, this was a single-institution study. Finally, we did not have histologic confirmation of imaging findings. Although all patients were biopsy-proven to have metastatic ILC, we cannot guarantee that each avid focus was a site of malignancy. However, ^{18}F-FES and ^{18}F-FDG PET/CT imaging findings were typical of findings for metastatic disease.

CONCLUSION

This retrospective review of prospective clinical trials using ^{18}F-FES PET/CT provides the first, to our knowledge, head-to-head comparison of ^{18}F-FES PET/CT and ^{18}F-FDG PET/CT in patients with metastatic ILC. ^{18}F-FES PET compares favorably with ^{18}F-FDG for identifying sites of metastatic disease, particularly osseous metastases. Because ILC is a malignancy in need of improved molecular imaging, larger trials are needed to evaluate the clinical value of ^{18}F-FES PET/CT in these patients.

DISCLOSURE

This work was supported by a Susan G. Komen for the Cure grant (KG110441 to Gary Ulaner) and an NIH/NCI Cancer Center support grant (P30 CA008748). No other potential conflict of interest relevant to this article was reported.

KEY POINTS

QUESTION: Does ^{18}F-FES PET/CT have value for evaluating disease in patients with lobular breast cancer?

PERTINENT FINDINGS: In this retrospective review of prospective clinical trials, ^{18}F-FES demonstrated both more metastatic lesions and higher SUVs for malignancy than did ^{18}F-FDG in 71% of patients.

IMPLICATIONS FOR PATIENT CARE: Our results warrant larger prospective trials of ^{18}F-FES PET/CT in ILC to evaluate potential added clinical value in patients with ILC.

REFERENCES

1. NCCN clinical practice guidelines in oncology: breast cancer—version 6.2020. NCCN website. https://www.nccn.org/professionals/physician_gls/pdf/breast.pdf. Published September 8, 2020. Accessed October 28, 2020.
2. Hildebrandt MG, Gerke O, Baun C, et al. [^{18}F]fluorodeoxyglucose (FDG)-positron emission tomography (PET)/computed tomography (CT) in suspected recurrent breast cancer: a prospective comparative study of dual-time-point FDG-PET/CT, contrast-enhanced CT, and bone scintigraphy. *J Clin Oncol.* 2016;34:1889–1897.
3. Li CI, Anderson BO, Daling JR, Moe RE. Trends in incidence rates of invasive lobular and ductal breast carcinoma. *JAMA.* 2003;289:1421–1424.
4. Li CI, Uribe DJ, Daling JR. Clinical characteristics of different histologic types of breast cancer. *Br J Cancer.* 2005;93:1046–1052.
5. Ciriello G, Gatza ML, Beck AH, et al. Comprehensive molecular portraits of invasive lobular breast cancer. *Cell.* 2015;163:506–519.
6. Pestalozzi BC, Zahrieh D, Mallon E, et al. Distinct clinical and prognostic features of infiltrating lobular carcinoma of the breast: combined results of 15 International Breast Cancer Study Group clinical trials. *J Clin Oncol.* 2008;26:3006–3014.
7. Yoder BJ, Wilkinson EJ, Massoll NA. Molecular and morphologic distinctions between infiltrating ductal and lobular carcinoma of the breast. *Breast J.* 2007;13:172–179.
8. Bertucci F, Orsetti B, Negre V, et al. Lobular and ductal carcinomas of the breast have distinct genomic and expression profiles. *Oncogene.* 2008;27:5359–5372.
9. Berg WA, Gutierrez L, NessAiver MS, et al. Diagnostic accuracy of mammography, clinical examination, US, and MR imaging in preoperative assessment of breast cancer. *Radiology.* 2004;233:830–849.
10. Lopez JK, Bassett LW. Invasive lobular carcinoma of the breast: spectrum of mammographic, US, and MR imaging findings. *Radiographics.* 2009;29:165–176.
11. Avril N, Rose CA, Schelling M, et al. Breast imaging with positron emission tomography and fluorine-18 fluorodeoxyglucose: use and limitations. *J Clin Oncol.* 2000;18:3495–3502.
12. Avril N, Menzel M, Dose J, et al. Glucose metabolism of breast cancer assessed by ^{18}F-FDG PET: histologic and immunohistochemical tissue analysis. *J Nucl Med.* 2001;42:9–16.
13. Bos R, van Der Hoeven JJ, van Der Wall E, et al. Biologic correlates of ^{18}fluorodeoxyglucose uptake in human breast cancer measured by positron emission tomography. *J Clin Oncol.* 2002;20:379–387.
14. Buck A, Schirrmeister H, Kuhn T, et al. FDG uptake in breast cancer: correlation with biological and clinical prognostic parameters. *Eur J Nucl Med Mol Imaging.* 2002;29:1317–1323.
15. Dashevsky BZ, Goldman DA, Parsons M, et al. Appearance of untreated bone metastases from breast cancer on FDG PET/CT: importance of histologic subtype. *Eur J Nucl Med Mol Imaging.* 2015;42:1666–1673.
16. Hogan MP, Goldman DA, Dashevsky B, et al. Comparison of ^{18}F-FDG PET/CT for systemic staging of newly diagnosed invasive lobular carcinoma versus invasive ductal carcinoma. *J Nucl Med.* 2015;56:1674–1680.
17. Lamovec J, Bracko M. Metastatic pattern of infiltrating lobular carcinoma of the breast: an autopsy study. *J Surg Oncol.* 1991;48:28–33.
18. Borst MJ, Ingold JA. Metastatic patterns of invasive lobular versus invasive ductal carcinoma of the breast. *Surgery.* 1993;114:637–641.
19. He H, Gonzalez A, Robinson E, Yang WT. Distant metastatic disease manifestations in infiltrating lobular carcinoma of the breast. *AJR.* 2014;202:1140–1148.
20. Kane AJ, Wang ZJ, Qayyum A, Yeh BM, Webb EM, Coakley FV. Frequency and etiology of unexplained bilateral hydronephrosis in patients with breast cancer: results of a longitudinal CT study. *Clin Imaging.* 2012;36:263–266.
21. Chen Z, Yang J, Li S, et al. Invasive lobular carcinoma of the breast: a special histological type compared with invasive ductal carcinoma. *PLoS One.* 2017;12:e0182397.
22. McCart Reed AE, Kutasovic JR, Lakhani SR, Simpson PT. Invasive lobular carcinoma of the breast: morphology, biomarkers and 'omics. *Breast Cancer Res.* 2015;17:12.
23. Kurland BF, Peterson LM, Lee JH, et al. Estrogen receptor binding (^{18}F-FES PET) and glycolytic activity (^{18}F-FDG PET) predict progression-free survival on endocrine therapy in patients with ER+ breast cancer. *Clin Cancer Res.* 2017;23:407–415.
24. van Kruchten M, de Vries EGE, Brown M, et al. PET imaging of oestrogen receptors in patients with breast cancer. *Lancet Oncol.* 2013;14:e465–e475.
25. Kurland BF, Peterson LM, Lee JH, et al. Between-patient and within-patient (site-to-site) variability in estrogen receptor binding, measured in vivo by ^{18}F-fluoroestradiol PET. *J Nucl Med.* 2011;52:1541–1549.
26. Sundararajan L, Linden HM, Link JM, Krohn KA, Mankoff DA. ^{18}F-fluoroestradiol. *Semin Nucl Med.* 2007;37:470–476.
27. Linden HM, Peterson LM, Fowler AM. Clinical potential of estrogen and progesterone receptor imaging. *PET Clin.* 2018;13:415–422.
28. Dehdashti F, Mortimer JE, Trinkaus K, et al. PET-based estradiol challenge as a predictive biomarker of response to endocrine therapy in women with estrogen-receptor-positive breast cancer. *Breast Cancer Res Treat.* 2009;113:509–517.
29. Peterson LM, Kurland BF, Schubert EK, et al. A phase 2 study of 16α-[^{18}F]-fluoro-17β-estradiol positron emission tomography (FES-PET) as a marker of hormone sensitivity in metastatic breast cancer (MBC). *Mol Imaging Biol.* 2014;16:431–440.
30. van Kruchten M, Glaudemans A, de Vries EFJ, Schroder CP, de Vries EGE, Hospers GAP. Positron emission tomography of tumour [^{18}F]fluoroestradiol uptake in patients with acquired hormone-resistant metastatic breast cancer prior to oestradiol therapy. *Eur J Nucl Med Mol Imaging.* 2015;42:1674–1681.
31. Ulaner GA, Riedl CC, Dickler MN, Jhaveri K, Pandit-Taskar N, Weber W. Molecular imaging of biomarkers in breast cancer. *J Nucl Med.* 2016;57(suppl 1):53S–59S.

32. Currin E, Peterson LM, Schubert EK, et al. Temporal heterogeneity of estrogen receptor expression in bone-dominant breast cancer: ^{18}F-fluoroestradiol PET imaging shows return of ER expression. *J Natl Compr Canc Netw.* 2016;14:144–147.
33. Nienhuis HH, van Kruchten M, Elias SG, et al. ^{18}F-fluoroestradiol tumor uptake is heterogeneous and influenced by site of metastasis in breast cancer patients. *J Nucl Med.* 2018;59:1212–1218.
34. Linden HM, Kurland BF, Peterson LM, et al. Fluoroestradiol positron emission tomography reveals differences in pharmacodynamics of aromatase inhibitors, tamoxifen, and fulvestrant in patients with metastatic breast cancer. *Clin Cancer Res.* 2011;17:4799–4805.
35. van Kruchten M, de Vries EG, Glaudemans AW, et al. Measuring residual estrogen receptor availability during fulvestrant therapy in patients with metastatic breast cancer. *Cancer Discov.* 2015;5:72–81.
36. Wang Y, Ayres KL, Goldman DA, et al. ^{18}F-fluoroestradiol PET/CT measurement of estrogen receptor suppression during a phase I trial of the novel estrogen receptor-targeted therapeutic GDC-0810: using an imaging biomarker to guide drug dosage in subsequent trials. *Clin Cancer Res.* 2017;23:3053–3060.
37. Knott K, Gratz D, Hubner S, Juttler S, Zankl C, Muller M. Simplified and automatic one-pot synthesis of 16α-[^{18}F]fluoroestradiol without high-performance liquid chromatography purification. *J Labelled Comp Radiopharm.* 2011;54:749–753.
38. Eheman CR, Shaw KM, Ryerson AB, Miller JW, Ajani UA, White MC. The changing incidence of in situ and invasive ductal and lobular breast carcinomas: United States, 1999-2004. *Cancer Epidemiol Biomarkers Prev.* 2009;18:1763–1769.
39. Siegel RL, Miller KD, Jemal A. Cancer statistics, 2020. *CA Cancer J Clin.* 2020;70:7–30.
40. Vinholes J, Coleman R, Eastell R. Effects of bone metastases on bone metabolism: implications for diagnosis, imaging and assessment of response to cancer treatment. *Cancer Treat Rev.* 1996;22:289–331.
41. Iagaru A, Minamimoto R. Nuclear medicine imaging techniques for detection of skeletal metastases in breast cancer. *PET Clin.* 2018;13:383–393.
42. Peterson LM, O'Sullivan J, Wu QV, et al. Prospective study of serial ^{18}F-FDG PET and ^{18}F-fluoride PET to predict time to skeletal-related events, time to progression, and survival in patients with bone-dominant metastatic breast cancer. *J Nucl Med.* 2018;59:1823–1830.
43. Eisenhauer EA, Therasse P, Bogaerts J, et al. New response evaluation criteria in solid tumours: revised RECIST guideline (version 1.1). *Eur J Cancer.* 2009;45:228–247.
44. Winston CB, Hadar O, Teitcher JB, et al. Metastatic lobular carcinoma of the breast: patterns of spread in the chest, abdomen, and pelvis on CT. *AJR.* 2000;175:795–800.
45. Ulaner GA, Saura C, Piha-Paul SA, et al. Impact of FDG PET imaging for expanding patient eligibility and measuring treatment response in a genome-driven basket trial of the pan-HER kinase inhibitor, neratinib. *Clin Cancer Res.* 2019;25:7381–7387.
46. Ulaner GA, Goldman DA, Gonen M, et al. Initial results of a prospective clinical trial of ^{18}F-fluciclovine PET/CT in newly diagnosed invasive ductal and invasive lobular breast cancers. *J Nucl Med.* 2016;57:1350–1356.
47. Tade FI, Cohen MA, Styblo TM, et al. Anti-3-^{18}F-FACBC (^{18}F-fluciclovine) PET/CT of breast cancer: an exploratory study. *J Nucl Med.* 2016;57:1357–1363.
48. Ulaner GA, Goldman DA, Corben A, et al. Prospective clinical trial of ^{18}F-fluciclovine PET/CT for determining the response to neoadjuvant therapy in invasive ductal and invasive lobular breast cancers. *J Nucl Med.* 2017;58:1037–1042.